Experimental evidence for a light and broad scalar resonance in $D^+ \to \pi^-\pi^+\pi^+$ decay .

E. M. Aitala,[9] S. Amato,[1] J. C. Anjos,[1] J. A. Appel,[5] D. Ashery,[14] S. Banerjee,[5] I. Bediaga,[1] G. Blaylock,[8] S. B. Bracker,[15] P. R. Burchat,[13] R. A. Burnstein,[6] T. Carter,[5] H. S. Carvalho,[1] N. K. Copty,[12] L. M. Cremaldi,[9] C. Darling,[18] K. Denisenko,[5] S. Devmal,[3] A. Fernandez,[11] G. F. Fox,[12] P. Gagnon,[2] C. Gobel,[1] K. Gounder,[9] A. M. Halling,[5] G. Herrera,[4] G. Hurvits,[14] C. James,[5] P. A. Kasper,[6] S. Kwan,[5] D. C. Langs,[12] J. Leslie,[2] B. Lundberg,[5] J. Magnin,[1] A. Massafferri,[1] S. MayTal-Beck,[14] B. Meadows,[3] J. R. T. de Mello Neto,[1] D. Mihalcea,[7] R. H. Milburn,[16] J. M. de Miranda,[1] A. Napier,[16] A. Nguyen,[7] A. B. d'Oliveira,[3,11] K. O'Shaughnessy,[2] K. C. Peng,[6] L. P. Perera,[3] M. V. Purohit,[12] B. Quinn,[9] S. Radeztsky,[17] A. Rafatian,[9] N. W. Reay,[7] J. J. Reidy,[9] A. C. dos Reis,[1] H. A. Rubin,[6] D. A. Sanders,[9] A. K. S. Santha,[3] A. F. S. Santoro,[1] A. J. Schwartz,[3] M. Sheaff,[17] R. A. Sidwell,[7] A. J. Slaughter,[18] M. D. Sokoloff,[3] J. Solano,[1] N. R. Stanton,[7] R. J. Stefanski,[5] K. Stenson,[17] D. J. Summers,[9] S. Takach,[18] K. Thorne,[5] A. K. Tripathi,[7] S. Watanabe,[17] R. Weiss-Babai,[14] J. Wiener,[10] N. Witchey,[7] E. Wolin,[18] S. M. Yang,[7] D. Yi,[9] S. Yoshida,[7] R. Zaliznyak,[13] and C. Zhang[7]

(Fermilab E791 Collaboration)

[1] *Centro Brasileiro de Pesquisas Físicas, Rio de Janeiro, Brazil,* [2] *University of California, Santa Cruz, California 95064,* [3] *University of Cincinnati, Cincinnati, Ohio 45221,* [4] *CINVESTAV, Mexico City, Mexico,* [5] *Fermilab, Batavia, Illinois 60510,* [6] *Illinois Institute of Technology, Chicago, Illinois 60616,* [7] *Kansas State University, Manhattan, Kansas 66506,* [8] *University of Massachusetts, Amherst, Massachusetts 01003,* [9] *University of Mississippi-Oxford, University, Mississippi 38677,* [10] *Princeton University, Princeton, New Jersey 08544,* [11] *Universidad Autonoma de Puebla, Puebla, Mexico,* [12] *University of South Carolina, Columbia, South Carolina 29208,* [13] *Stanford University, Stanford, California 94305,* [14] *Tel Aviv University, Tel Aviv, Israel,* [15] *Box 1290, Enderby, British Columbia, V0E 1V0, Canada,* [16] *Tufts University, Medford, Massachusetts 02155,* [17] *University of Wisconsin, Madison, Wisconsin 53706,* [18] *Yale University, New Haven, Connecticut 06511*

August, 2000

Abstract

From a sample of 1172 ± 61 $D^+ \to \pi^-\pi^+\pi^+$ decay, we find $\Gamma(D^+ \to \pi^-\pi^+\pi^+)/\Gamma(D^+ \to K^-\pi^+\pi^+) = 0.0311 \pm 0.0018^{+0.0016}_{-0.0026}$. Using a coherent amplitude analysis to fit the Dalitz plot of these decays, we find strong evidence that a scalar resonance of mass $478^{+24}_{-23} \pm 17$ MeV/c^2 and width $324^{+42}_{-40} \pm 21$ MeV/c^2 accounts for approximately half of all decays.

The three-body decays of charm mesons often proceed as quasi-two-body decays with resonant intermediate states. In our companion paper[1], we find that $D_s^+ \to f_0(980)\pi^+$ accounts for approximately half of the three-pion decay rate and $D_s^+ \to f_0(1370)\pi^+$ accounts for more than half of what remains, clearly establishing the dominance of isoscalar resonances in producing the three-pion final state. In this paper we present a study of the singly Cabibbo-suppressed decay $D^+ \to \pi^-\pi^+\pi^+$. We determine the ratio of decay rates $\Gamma(D^+ \to \pi^-\pi^+\pi^+)/\Gamma(D^+ \to K^-\pi^+\pi^+)$ and study the $D^+ \to \pi^-\pi^+\pi^+$ Dalitz plot to determine the structure of its density distribution. We find that allowing an amplitude for an additional scalar state, with mass and width unconstrained, improves our fit substantially. The mass and width of the resonance found by this fit are $478^{+24}_{-23} \pm 17$ MeV/c^2 and $324^{+42}_{-40} \pm 21$ MeV/c^2. Referring to this $\pi^+\pi^-$ resonance as the $\sigma(500)$, we find that $D^+ \to \sigma(500)\pi^+$ accounts for about half of the total decay rate.

Other experiments have presented controversial evidence for low-mass $\pi\pi$ resonances in partial wave analyses [2, 3, 4], with ambiguous results for the characteristics of such particles[5, 6]. Theoretically, light scalar and isoscalar resonances are predicted in models for spontaneous breaking of chiral symmetry such as the Nambu-Jona-Lasinio linear σ model [8] and its QCD extension [9]. Also, these particles have important consequences for the quark model [6], for quark-gluon models [7], for understanding low energy $\pi\pi$ interactions [10, 11], and for understanding the $\Delta I = 1/2$ rule[12].

This study is based on the sample of 2×10^{10} events recorded in Fermilab experiment E791, in which 500 GeV/c π^--nucleon interactions were observed using an open geometry spectrometer. The final analysis makes no direct use of particle identification; it is solely based on tracking and vertex reconstruction capabilities. To reduce background, we required a 3-prong decay (secondary) vertex to be well-separated from the production (primary) vertex, and located well outside of the target foils and other solid material. The momentum vector of the D candidate had to point back to the primary vertex. A more detailed description of the final sample selection criteria and some additional details are provided in the companion paper [1] where the resulting $\pi^-\pi^+\pi^+$ invariant mass distribution is shown as Fig. 1.

We have, in addition to the combinatorial background, three kinds of charm backgrounds: the reflection of the $D^+ \to K^-\pi^+\pi^+$ decay, located below 1.85 GeV/c^2 in this spectrum; the decay $D^0 \to K^-\pi^+$ plus one extra track (mostly from the primary vertex); and the decay chain $D_s^+ \to \eta'\pi^+$, $\eta' \to \rho^0(770)\gamma$, $\rho^0(770) \to \pi^+\pi^-$. The last two reflections populate the whole $\pi^-\pi^+\pi^+$ analyzed spectrum. We use Monte Carlo (MC) simulations and data to determine both the shape and the size of each type of charm background. The combinatorial background in the $\pi^-\pi^+\pi^+$ invariant mass spectrum is represented by an exponential function.

We fit the $\pi^-\pi^+\pi^+$ invariant mass distribution shown in Fig.1 of reference [1] as the sum of D^+ and D_s^+ signals plus background. Each signal is described as the sum of two Gaussians with a common centroid but different widths, all these parameters determined by the fit. The background is represented by a function with four terms described above and in [1]. The fit yields 1172 ± 61 D^+ events and 848 ± 44 D_s^+ events.

We measure the branching ratio for $D^+ \to \pi^-\pi^+\pi^+$ relative to that of $D^+ \to K^-\pi^+\pi^+$. The $K^-\pi^+\pi^+$ signal, selected with the same criteria used for the $\pi^-\pi^+\pi^+$ signal, is 34790 ± 232 events. The absolute efficiency, ε, for each decay mode is approximately 3%. From Monte Carlo studies we determine that the ratio $\varepsilon(D^+ \to \pi^-\pi^+\pi^+)/\varepsilon(D^+ \to K^-\pi^+\pi^+) = 1.08 \pm 0.02$. Note that we use the decay matrix element found in this analysis and an appropriate one for $D^+ \to K^-\pi^+\pi^+$ to determine the efficiencies. We also weight the MC production model to match our data. We find the relative branching ratio to be

$$\frac{\Gamma(D^+ \to \pi^-\pi^+\pi^+)}{\Gamma(D^+ \to K^-\pi^+\pi^+)} = 0.0311 \pm 0.0018^{+0.0016}_{-0.0026}\,. \tag{1}$$

The first error is statistical and the second is systematic. Uncertainties in the $\pi^-\pi^+\pi^+$ background shape and the levels of some contributions dominate the systematic error. This result can be compared with the measurements reported by E691 [13], $0.035 \pm 0.007 \pm 0.003$, by WA82 [14], $0.032 \pm 0.011 \pm 0.003$, and by E687 [15], $0.043 \pm 0.003 \pm 0.003$.

To study the resonant structure of the decay $D^+ \to \pi^-\pi^+\pi^+$, we consider the 1686 candidates with invariant mass between 1.85 and 1.89 GeV. The integrated signal-to-background ratio in this range is about 2:1. Fig. 1 shows the Dalitz plot for these events. The horizontal and vertical axes are the squares of the $\pi^+\pi^-$ invariant masses, and the plot has been symmetrized with respect to the two π^+'s.

To study the resonant structure in Fig. 1, we use MINUIT[16] to extract the parameters. We do this by maximizing the log (Likelihood) $\mathcal{L}$ for several models of signal and background. For each model we compute $\mathcal{L}$ in terms of signal and background probability distribution functions (PDF's) of the $\pi^-\pi^+\pi^+$ invariant mass, M, and the Lorentz invariants $s_{12} \equiv m_{12}^2$ and $s_{13} \equiv m_{13}^2$ (in our convention the odd-charged pion is labeled particle 1). Writing $\mathcal{P}_S$ and $\mathcal{P}_B$ for the signal and background PDF's, $\mathcal{L} = \prod_{j=1}^{1686}[\mathcal{P}_S + \mathcal{P}_B]_j$. We take $\mathcal{P}_S = \frac{1}{N_S} g(M)\varepsilon(s_{12}, s_{13}) \mid \mathcal{A} \mid^2$, with

$$\mathcal{A} = a_0 e^{i\delta_0}\mathcal{A}_0 + \sum_{n=1}^{N} a_n e^{i\delta_j}\mathcal{A}_n(s_{12}, s_{13})\,. \tag{2}$$

In this equation N_S is the normalization constant, $\varepsilon(s_{12}, s_{13})$ is the net efficiency, $g(M)$ is a Gaussian function describing the signal $\pi^-\pi^+\pi^+$ invariant mass spectrum.

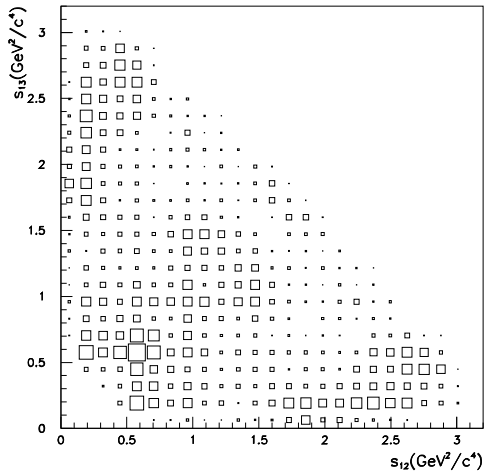

Figure 1: $D^+ \to \pi^-\pi^+\pi^+$ Dalitz plot distribution. Since we have two identical particles this distribution was symmetrized.

The fit parameters are the coefficient magnitudes, a_n, and the phases, δ_n.

The non-resonant amplitude, $\mathcal{A}_0$, is represented by a constant. Each resonant amplitude, $\mathcal{A}_n (n \geq 1)$, is written as a product of four terms.

$$\mathcal{A}_n = {}^J F_n \times {}^J \mathcal{M}_n \times BW_n \tag{3}$$

The first term is form factor for the n^{th} resonance We assume the form factor for the D decay to be one. ${}^J\mathcal{M}_n$ is a term which accounts for angular-momentum conservation and depends on the spin J of the resonance. The final term is a relativistic Breit-Wigner function given by:

$$BW_n = \frac{1}{m^2 - m_0^2 + i m_0 \Gamma_n(m)} \tag{4}$$

with

$$\Gamma(m) = \Gamma_0 \frac{m_0}{m} \left(\frac{p^*}{p_0^*} \right)^{2J+1} \frac{{}^J F_n^2(p^*)}{{}^J F_n^2(p_0^*)} \ . \tag{5}$$

In Eqs. 3 and 4, m is the invariant mass of the two pions forming a spin-J resonance. The functions ${}^J F$ are the Blatt-Weisskopf damping factors [17]: ${}^0 F = 1$ for spin 0 particles, ${}^1 F = 1/\sqrt{1 + (rp^*)^2}$ for spin 1 and ${}^2 F = 1/\sqrt{9 + 3(rp^*)^2 + (rp^*)^4}$ for spin

2. The parameter r is the radius of the resonance ($\sim 3fm$) [18] and $p^* = p^*(m)$ the momentum of decay particles at mass m, measured in the resonance rest frame, $p_0^* = p^*(m_0)$, where m_0 is the resonance mass. The spin part of the amplitude ${}^J\mathcal{M}_n$ is defined equal to 1 for a spin-0 resonance, $-2 \mid \mathbf{p_3} \mid\mid \mathbf{p_2} \mid cos\theta$ for spin-1 and $\frac{4}{3}(\mid \mathbf{p_3} \mid\mid \mathbf{p_2} \mid)^2(3cos^2\theta - 1)$, where $\mathbf{p_3}$ is the 3-momentum of the unlike-charge pion and $\mathbf{p_2}$ is the 3-momentum of the other like-charge pion, both measured in the resonance rest frame; and θ is the angle between pions 2 and 3. Finally, each resonant amplitude is Bose symmetrized: $\mathcal{A}_n = \mathcal{A}_n[(\mathbf{12})\mathbf{3}] + \mathcal{A}_n[(\mathbf{13})\mathbf{2}]$.

The background distribution is given by $\mathcal{P}_B = b(M)\sum_{i=1}^{3}\frac{b_i}{N_{B_i}}\mathcal{B}_i(s_{12}, s_{13})$; $b(M)$ is the function describing the background distribution in the $\pi^-\pi^+\pi^+$ spectrum, b_i are the relative amount of each background type and N_{B_i} are the corresponding normalization constants.

The three components of the background distribution are the combinatorial background, assumed to be uniform before any acceptance effects, and the $D^0 \to K^-\pi^+$ and $D_s^+ \to \eta'\pi^+$ reflections. The relative background fractions are $80 \pm 6\%$, $4 \pm 1\%$, and $16 \pm 6\%$, respectively. The shape, location, and size of the charm background were obtained using MC simulations and previously determined D^0 and D_s production rates relative to D^+ in our data sample. All parameters used for the background description are fixed during the fit.

The dominance of the above three background contributions was checked in several tests. The analysis was repeated with more stringent selection criteria, with various levels of Čerenkov-counter requirements on the pions, and with varied background levels in the fit. All test results were consistent with the quoted final results. In addition, Monte Carlo simulations were used to study specific charm decay channels and a generic sample of charm decays. The latter was examined to look for Dalitz-plot structure in the events which passed our final selection criteria. No structures, other than those noted above, were significant.

In a first model, which we will refer to as Fit 1, the signal PDF includes a non-resonant amplitude and amplitudes for D^+ decaying to a π^+ and any of five established $\pi^+\pi^-$ resonances[5]: $\rho^0(770)$, $f_0(980)$, $f_2(1270)$, $f_0(1370)$, and $\rho^0(1450)$. In the case of the $f_0(980)$ and $f_0(1370)$, we used the parameters of Ref. [1] and not those of Ref. [5]. The fit extracts the magnitudes and phases of each of the amplitudes along with the error matrix for these parameters. We calculate the decay fraction for each amplitude as its intensity, integrated over the Dalitz plot, divided by the integrated intensity of the signal's coherently summed amplitudes. The Fit 1 results are listed in the first column of Table 1. In this model, the non-resonant, the $\rho^0(1450)\pi^+$ and the $\rho^0(770)\pi^+$ amplitudes dominate. The qualitative features of this fit are similar to those reported by E691[13] and E687[15].

mode	Fit 1 Fraction(%) Magnitude Phase	Fit 2 Fraction(%) Magnitude Phase
$\sigma\pi^+$	–	$46.3 \pm 9.0 \pm 2.1$
	–	$1.17 \pm 0.13 \pm 0.06$
	–	$(205.7 \pm 8.0 \pm 5.2)^\circ$
$\rho^0(770)\pi^+$	20.8 ± 2.4	$33.6 \pm 3.2 \pm 2.2$
	1(fixed)	1(fixed)
	0(fixed)	0(fixed)
NR	38.6 ± 9.7	$7.8 \pm 6.0 \pm 2.7$
	1.36 ± 0.20	$0.48 \pm 0.18 \pm 0.09$
	$(150.1 \pm 11.5)^\circ$	$(57.3 \pm 19.5 \pm 5.7)^\circ$
$f_0(980)\pi^+$	7.4 ± 1.4	$6.2 \pm 1.3 \pm 0.4$
	0.60 ± 0.07	$0.43 \pm 0.05 \pm 0.02$
	$(151.8 \pm 16.0)^\circ$	$(165.0 \pm 10.9 \pm 3.4)^\circ$
$f_2(1270)\pi^+$	6.3 ± 1.9	$19.4 \pm 2.5 \pm 0.4$
	0.55 ± 0.08	$0.76 \pm 0.06 \pm 0.03$
	$(102.6 \pm 16.0)^\circ$	$(57.3 \pm 7.5 \pm 2.9)^\circ$
$f_0(1370)\pi^+$	10.7 ± 3.1	$2.3 \pm 1.5 \pm 0.8$
	0.72 ± 0.12	$0.26 \pm 0.09 \pm 0.03$
	$(143.2 \pm 9.7)^\circ$	$(105.4 \pm 17.8 \pm 0.6)^\circ$
$\rho^0(1450)\pi^+$	22.6 ± 3.7	$0.7 \pm 0.7 \pm 0.3$
	1.04 ± 0.12	$0.14 \pm 0.07 \pm 0.02$
	$(45.8 \pm 14.9)^\circ$	$(319.1 \pm 39.0 \pm 10.9)^\circ$

Table 1: Final result with the first errors statistical and the second, in Fit 2, the systematic.

To assess the quality of the fit, we developed a fast-MC program which produces binned Dalitz-plot densities accounting for signal and background PDF's, including detector efficiency and resolution. Comparing the binned Dalitz-plot-density distribution generated by MC events using the magnitudes and phases of the amplitudes given in Fit 1 with that for the data, we produce the χ^2 distribution for the difference in densities and observe a concentration of a large χ^2 in the low $\pi^+\pi^-$ mass ($m_{\pi^+\pi^-}$) region. The χ^2 summed over all bins is 254 for 162 degrees of freedom (ν), which corresponds to a confidence level less than 10^{-5}, assuming Gaussian errors. Since the two $m^2_{\pi^+\pi^-}$ projections are nearly independent, we display the sum of s_{12} and s_{13} in Fig. 2a for the data and for the fast-MC.

The small value of the confidence level casts doubt on the validity of the model used. While the projection of the MC onto the $\pi^+\pi^-$ mass^2 axis describes the data in the $\rho^0(770)$ and $f_0(980)$ regions well, there is a discrepancy at lower mass, suggesting the possibility of another amplitude.

To investigate the possibility that another $\pi^+\pi^-$ resonance contributes an amplitude to the $D^+ \to \pi^-\pi^+\pi^+$ decay, we add a sixth resonant amplitude to the signal PDF. We allow its mass and width to float and assume a scalar angular distribution. This fit (Fit 2) converges and finds values of 478^{+24}_{-23} MeV/c^2 for the mass and 324^{+42}_{-40} MeV/c^2 for the width. We will refer to this possible state as the $\sigma(500)$. The corresponding results, including the systematic errors [1], are collected in the second column of Table 1.

In Fit 2, the $\sigma(500)$ amplitude produces the largest decay fraction, 46%, with a relatively small statistical error, 9%. The non-resonant fraction, which at (39 ± 10)% was the largest in the original fit, is now only (8 ± 6)%. When we project this model onto the Dalitz plot, the χ^2/ν becomes 138/162. The projection of this model onto the $\pi^+\pi^-$ invariant mass squared distribution, shown in Fig. 2b, describes the data well, including the accumulation of events near 0.2 GeV$^2/c^4$. We tested the accuracy of the fit's error estimates by producing hundreds of fast-MC samples using the parameters of Fit 2 and then fitting the samples. The central values of all the parameters are reproduced accurately, and the width of the $\sigma(500)$ fraction distribution is 0.12, slightly larger than MINUIT's estimate, 0.09.

When comparing the two models we used the fast-MC to simulate an ensemble of samples for each model. For each sample we calculated $\Delta w = -2(\ln \mathcal{L}_i - \ln \mathcal{L}_\sigma)$, where $\mathcal{L}_\sigma$ and $\mathcal{L}_i$ are the likelihood functions evaluated with the parameters from the fit with and without the $\sigma\pi^+$ amplitude, respectively. In the data, $\Delta w = 118$; in the fast MC with a σ, $\langle \Delta w \rangle = 108$; in the fast MC with no σ, $\langle \Delta w \rangle = -106$. In both MC experiments, the rms deviation for Δw is about 20, indicating a strong

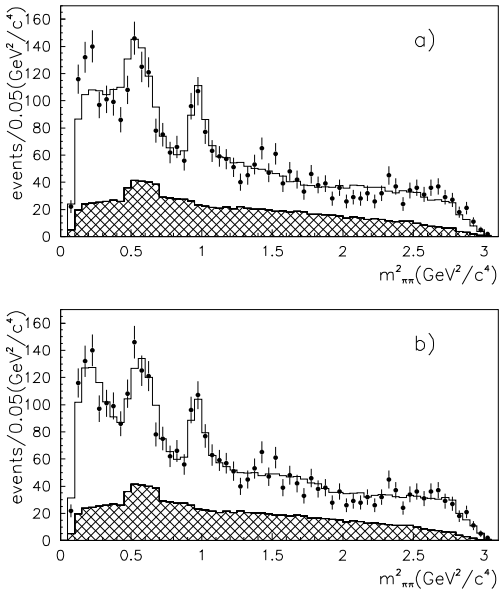

Figure 2: s_{12} and s_{13} projections for data (error bars) and fast-MC (solid). The shaded area is the background distribution, (a) solution with the Fit 1, (b) solution with Fit 2.

preference for the additional amplitude, as is indicated also by the difference in χ^2/ν for the two models.

We consider the systematic errors associated with the values of the fixed parameters in the fit. The most important ones come from uncertainties in the background model (the background shape, composition, and level), in particular the $D_s^+ \to \eta'\pi^+$ reflection which populates the same region as the $D^+ \to \rho^0\pi^+$ component. We also account for the uncertainties in the parameters describing the acceptance function.

To better understand our data, we also fit it with vector, tensor, and toy models for the sixth (sigma) amplitude, allowing the masses, widths, and relative amplitudes to float freely. The vector and tensor models test the angular distribution of the signal. The toy model tests the phase variation expected of a Breit-Wigner amplitude by substituting a constant relative phase. The vector resonance model converges to poorly defined values of the mass and width: 805 ± 194 MeV/c^2 and 1438 ± 903 MeV/c^2; the tensor model to more poorly defined values: 2350 ± 683 MeV/c^2 and -690 ± 1033; and the toy model to 434 ± 11 MeV/c^2 and 267 ± 37 MeV/c^2. As

a test of the models, we again project the vector, tensor, and toy models onto the Dalitz plot and obtain $\chi^2/\nu = 188/162$, 148/162, and 152/162, respectively. For these models, we also find $\Delta w = 66$, 13, and 15 where MC experiments predict $\langle \Delta w \rangle \approx 64$, 56, and 38 when the data is generated with the scalar parameters and the negatives of those values when the MC data is generated according to the vector, tensor, and toy model parameters. The rms widths of the MC distributions are 15, 15, and 11 units respectively. These statistical tests strongly exclude the vector model. They clearly prefer the scalar model to the tensor and toy models. Note that the central value for the tensor mass is well above threshold for D^+ decay and the negative width is an indication that no physically meaningful tensor resonance fits the data. In the toy model, the extra amplitude interferes strongly with a large non-resonant amplitude, leading to an unphysically large sum of resonant fractions.

In summary, from 1172 ± 61 $D^+ \to \pi^-\pi^+\pi^+$ we have measured $\Gamma(D^+ \to \pi^-\pi^+\pi^+)/\Gamma(D^+ \to K^-\pi^+\pi^+) = 0.0311 \pm 0.0018^{+0.0016}_{-0.0026}$. In an amplitude analysis of a sample with S:B $\approx$ 2:1 we find strong evidence that a scalar resonance with mass $478^{+24}_{-23} \pm 17$ MeV/c^2 and width $324^{+42}_{-40} \pm 21$ MeV/c^2 produces a decay fraction $\approx 50\%$. Alternative explanations of the data fail to describe it as well. The prominence of an amplitude for an isoscalar plus a π^+ in this decay accords well with our observation that the amplitude for an isoscalar plus a pion produce a large majority of all $D_s^+ \to \pi^-\pi^+\pi^+$ decays[1].

We gratefully acknowledge the assistance of the staffs of Fermilab and of all the participating institutions. This research was supported by the Brazilian Conselho Nacional de Desenvolvimento Científico e Tecnológico, CONACyT (Mexico), the Israeli Academy of Sciences and Humanities, the U.S. Department of Energy, the U.S.-Israel Binational Science Foundation, and the U.S. National Science Foundation. Fermilab is operated by the Universities Research Association, Inc., under contract with the U.S. Department of Energy.

References

[1] E791 Collaboration, E.M. Aitala et al, "Study of the $D_s^+ \to \pi^-\pi^+\pi^+$ decay and measurement of f_0 masses and widths " (Preceding paper).

[2] WA102 Collaboration, D. Barberis, *et al.*, Phys. Lett. B **453**,316 (1999).

[3] CLEO Collaboration, D.M. Asner *et al.*, Phys Rev D**61**,012002 (2000)

[4] GAMS Collaboration, D. Alde, *et al.*, Phys. Lett. B**397** , 350 (1997).

[5] Particle Data Group, C. Caso *et al.*, Eur. Phys. Jour. C **3**, 1 (1998).

[6] N. Tornqvist, hep-ph 9904346.

[7] S. Narison, Nucl. Phys. B**509**, 312 (1998)

[8] Y. Nambu and G. Jona-Lasinio, Phys. Rev. **122**, 345 (1961).

[9] R. Delburgo and M.D. Scadron, Phys. Rev. Lett **48**, 379 (1982).

[10] K. Erkelene, Phys. Rep. C **13**, 190 (1974).

[11] M.R. Pennington, hep-ph/9905241.

[12] T. Morozumi, C.S. Lim, and A.I. Sanda, Phy. Rev. Lett. **65**, 404 (1990).

[13] E691 Collaboration, J. Anjos *et al.*, Phy.Rev.Lett. **62**, 125 (1989).

[14] WA82 Collaboration, M. Adamovich *et al.*, Phys. Lett. B **305**, 177 (1993).

[15] E687 Collaboration, P.L. Frabetti *et al.*, Phys. Lett. B **407**, 79 (1997).

[16] F. James,"MINUIT, Function Minimization and Error Analysis", CERN Program Library Long Write-up D506 (1994).

[17] J.M. Blatt and V.F. Weisskopf, Theoretical Nuclear Physics, John Wiley & Sons, New York, 1952.

[18] ARGUS Collaboration, H. Albrecht *et al.*, Phys. Lett. B **308**, 435(1993).